Magnetic sensing via ultrasonic excitation

Hisato Yamada,[1] Kazuya Takashima,[1] Kenji Ikushima,[1,a)] Hiraku Toida,[2] Michitaka Sato,[3] and Yoshiichi Ishizawa[3]
[1]*Department of Applied Physics, Tokyo University of Agriculture and Technology, Nakacho, Koganei, Tokyo 184-8588, Japan*
[2]*Department of Basic Science, University of Tokyo, Komaba, Meguro-ku, Tokyo 153-8902, Japan*
[3]*JFE Techno-Research Corporation, Kawasaki-ku, Kawasaki 210-0855, Japan*

(Received 25 March 2013; accepted 16 April 2013; published online 30 April 2013)

We present ultrasonic techniques for magnetic measurements. Acoustically modulated magnetization is investigated with sensitive rf detection by narrowband loop antennas. Magnetization on the surface of ferromagnetic metals is temporally modulated with the rf frequency of the irradiated ultrasonic waves, and the near-field components emitted from the focal point of the ultrasonic beam are detected. Based on the principle of the acoustically stimulated electromagnetic (ASEM) response, magnetic sensing and tomography are demonstrated by ultrasonic scanning. We show that ASEM imaging combines good acoustic resolution with magnetic contrast. The sensitivity of this method is estimated to be about 6 G/Hz$^{1/2}$ in our current setup. © *2013 AIP Publishing LLC*. [http://dx.doi.org/10.1063/1.4803188]

I. INTRODUCTION

The magnetic characteristics of materials have been imaged by a variety of techniques, including conventional contact methods with sensitive magnetic field sensors,[1–3] electron microscopy techniques in which modification of electron motion by the Lorentz force is detected,[4] and optical methods which exploit the Kerr effect.[5] Scanning a surface with a sensitive magnetic field sensor provides direct information on the material surface, although it is generally difficult to maintain contact with rough surfaces and the technique is not suitable for environments subjected to magnetic fields. The electron microscopy and optical techniques require substantial equipment and are thus limited to laboratory use. Here we present a more convenient alternative magnetic sensing combined with ultrasonic inspection.

Ultrasonic waves can propagate through optically opaque substances, such as the human body, metals, and concrete. The majority of existing ultrasonic techniques are restricted to determining the mechanical properties of materials from the elasticity or mass density of the target. Recently, a method for measuring electromagnetic properties through acoustic-wave coupling has been reported.[6] In this method, the acoustically stimulated electromagnetic (ASEM) response is detected by a narrowband antenna tuned to the center frequency of the incident ultrasonic waves.

A major advantage of the ASEM method is that it is compatible with conventional ultrasonic pulse-echo sensing, and can be used for evaluating the electromagnetic properties of a material detected by the pulse-echo inspection. In this paper, we demonstrate how magnetic properties can be assessed by measuring the ASEM response. First, the characteristics of rf magnetic fields induced by longitudinal acoustic excitation are investigated in a typical ferromagnet (a commercial ferrite, $SrO/6Fe_2O_3$). In fundamental experiments, a proper antenna configuration is determined and different magnetic materials are selectively imaged. We also present an example of the complementary use of the ASEM method with ultrasonic tomography. Finally, as one example of practical use, the strain-induced martensitic transformation[7] in an austenitic stainless steel (SUS304) is studied by using the ASEM method. We have confirmed that the ASEM intensity is strongly correlated with the magnitude of the surface magnetic flux density induced by external stress.

II. THEORETICAL BACKGROUND

Biased magnetostriction is phenomenologically equivalent to piezomagnetism in the linear response regime, and we will make no distinction between them for the purpose of this discussion.[8] Under adiabatic conditions, the applicable mechanical and magnetic equations of state for the piezomagnetic medium can be written as ($i, j = 1, 2, 3$ and $m, n = 1, 2, \ldots 6$)

$$\begin{aligned} S_m &= s_{mn} T_n + d_{jm} H_j, \\ B_j &= d_{jm} T_m + \mu_{ji} H_j, \end{aligned} \tag{1}$$

where the S, T, H, and B are the strain, stress, magnetic field, and magnetic flux density components, respectively. The coefficients relating these quantities, s, d, and μ, are the elastic compliance, the piezomagnetic constant, and permeability constant, respectively. The magnetic flux density, $\boldsymbol{B}(t)$, is temporally modulated through Eq. (1) when the strain, $\boldsymbol{T}(t)$, is applied through acoustic irradiation. It follows that the magnetic dipole moment averaged in the acoustically excited area, $\boldsymbol{m}(t) \propto \boldsymbol{B}(t)$, oscillates at the frequency of the acoustic waves. The magnetic flux density emitted to the surrounding

a)Electronic mail: ikushima@cc.tuat.ac.jp

 © 2013 AIP Publishing LLC

Downloaded 02 May 2013 to 142.51.1.212. This article is copyrighted as indicated in the abstract. Reuse of AIP content is subject to the terms at: http://rsi.aip.org/about/rights_and_permissions

environment is then expressed by the following formula:[9]

$$\boldsymbol{B}_{\text{emit}}(\boldsymbol{x},t) = -\frac{\mu_0}{4\pi}\left\{\frac{3(\boldsymbol{m}\cdot\boldsymbol{n_0})\boldsymbol{n_0}-\boldsymbol{m}}{r^3} + \frac{3(\dot{\boldsymbol{m}}\cdot\boldsymbol{n_0})\boldsymbol{n_0}-\dot{\boldsymbol{m}})}{cr^2} + \frac{(\ddot{\boldsymbol{m}}\times\boldsymbol{n_0})\times\boldsymbol{n_0}}{c^2 r}\right\}, \quad (2)$$

where the $\boldsymbol{x} = \boldsymbol{n}_0 r$ represents a vector from the position of the magnetic dipole moment to the observation point with a distance of r, μ_0 is the space permeability, and c is the speed of light. In Eq. (2), the first term represents the near-field component, the second term represents the intermediate component, and the last term corresponds to the magnetic-dipole radiation produced by the acoustic waves.

Because the distance, r, is much smaller than the wavelength of the EM waves in our experiments, we focus on the near-field term. For the sinusoidal oscillation of the acoustically excited magnetic dipole moment, $\boldsymbol{m}(t) = \boldsymbol{m}_0 \sin\omega t$, Eq. (2) can be written as

$$\boldsymbol{B}^{\text{near}}_{\text{emit}}(\boldsymbol{x},t) = -\frac{\mu_0}{4\pi}\{3(\boldsymbol{m}_0\cdot\boldsymbol{n_0})\boldsymbol{n_0}-\boldsymbol{m}_0\} \times \frac{\sin\omega t}{r^3}. \quad (3)$$

Supposing that $\boldsymbol{H}$, $\boldsymbol{B}$, and $\boldsymbol{m}$ are axial vectors parallel to the 3-axis in ferromagnetic materials, the non-zero piezomagnetic constants will be limited to $d_{31} = d_{32}$ and d_{33}[8] in the uniaxial symmetry of a polycrystalline medium. Therefore, the B_3 component will be temporally modulated. Thus the voltage, V_{sig}, detected by a loop antenna (or a coil) will be $V_{\text{sig}} \propto \{3(\boldsymbol{m}_0\cdot\boldsymbol{n_0})\boldsymbol{n_0}-\boldsymbol{m}_0)\omega\cos\omega t\}/r^3$. Consequently, the signal intensity is proportional to r^{-3} and ω, and is strongly affected by the geometric configuration of the antennas.

III. EXPERIMENTAL SETUP

The experimental setup for the ASEM measurements is shown in Fig. 1(a). A target sample is placed in the focused zone about 60 mm from a 10 MHz ultrasonic transducer (diameter 15 mm), to which rectangular 50 ns wide pulses are applied by a pulser/receiver (Panametrics-NDT, 5077PR). The appropriate distance between the sample and the transducer allows us to temporally separate the pulsed ASEM response from the EM noise generated by the transducer. The ASEM response is obtained at half the echo delay time, t_{echo}, and is detected by a narrowband loop antenna tuned into the center frequency of the ultrasonic waves with a bandwidth of about 200 kHz.[6] Signals picked up by the antenna are fed to a low-noise preamplifier (NF, SA-230F5), and averaged by using digital oscilloscopes or high-speed digitizers. Spatial images of the ASEM response are obtained by mechanically scanning the focused ultrasonic beam. The focused spot is estimated to have a diameter of about 0.7 mm by using a micro hydrophone. The magnetic flux density is measured by a calibrated Hall sensor (SHS 371).

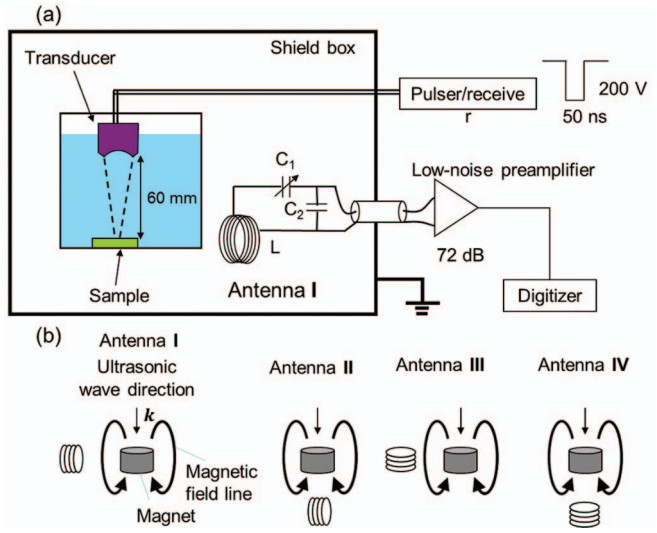

FIG. 1. (a) Schematic of the experimental setup for the ASEM method. (b) Four geometric configurations of a loop antenna for the magnetic field lines and the incident ultrasonic wave vector.

IV. ASEM RESPONSE OF FERRITE MAGNETS

The basic properties of the ASEM response in ferromagnetic materials are studied for commercial cylindrical ferrite magnets ($SrO/6Fe_2O_3$, 20 mm diameter, thickness $h = 5$ and 10 mm). The geometric configurations of the antenna (I, II, III, and IV) for the specimen and the incident ultrasonic wave vector, $\boldsymbol{k}$, are shown in Fig. 1(b). The distance between the antenna and the specimen is about 35 mm. The ultrasonic focal spot is on the center of the upper surface of the specimen. Figure 2(a) shows a typical real-time waveform of ASEM response from the ferrite. The two apparent signals coincident with the excitation ($t = 0$ μs) and the ultrasonic pulse-echo ($t_{\text{echo}} = 80$ μs) signals are attributed to the EM waves generated by the transducer. In addition, a weaker EM signal of about 0.3 μV occurs at the middle point ($t_{\text{echo}}/2 = 40$ μs)

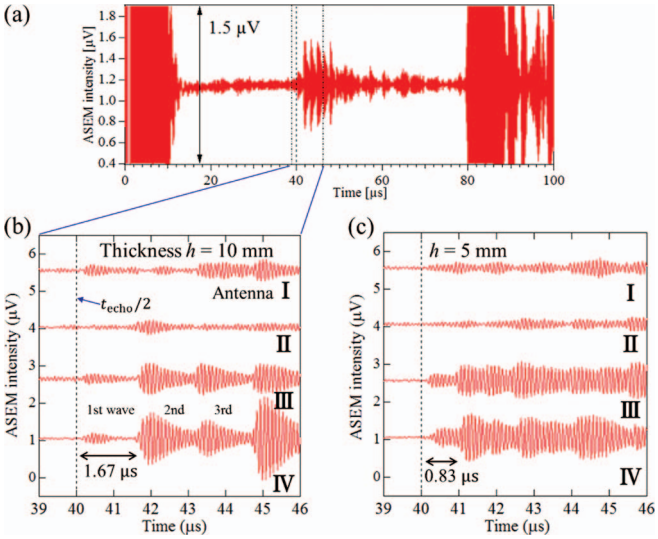

FIG. 2. (a) Typical real-time waveform of the ASEM response measured by Antenna III. The detailed waveforms for the (b) 10 mm and (c) 5 mm thick specimens.

Downloaded 02 May 2013 to 142.51.1.212. This article is copyrighted as indicated in the abstract. Reuse of AIP content is subject to the terms at: http://rsi.aip.org/about/rights_and_permissions

between the excitation and pulse-echo signals. This weaker signal is identified as the ASEM response emitted by the ferrite magnet. ASEM signals with durations much longer than the excitation pulse width (about 50 ns) are observed, indicating that ultrasonic waves are well confined in the specimen. The enlarged view of the waveforms (Figs. 2(b) and 2(c)) reveals a comb-like periodic feature. For metallic ferrite, the rf fields should be generated on only the surface of the specimen. Therefore, the comb-like structure is interpreted as a multiple reflection of ultrasonic waves at the front and the back faces of the specimen. The period of the ASEM response for the 10-mm-thick specimen is estimated to be 1.67μs (arrow in Fig. 2(b)). Because the velocities of the longitudinal and transversal waves are about 6 and 3.5 km/s, respectively, the longitudinal waves travel between the front and the back faces of the specimen. The experiments using the 5-mm-thick specimen support our interpretation (Fig. 2(c)). The geometric configuration of antenna also affects the signal intensities. The ASEM intensities measured with Antenna III and IV are much larger than those measured with Antenna I and II; Antenna III and IV measure the rf magnetic fields parallel to the static magnetic flux vectors originating from the magnetization of ferrite. This means that the acoustic excitation predominately induce the temporal amplitude modulation of the magnetization through $B_3(t) = d_{3m}T_m(t)$, as described in Sec. II.

There are two properties of the ASEM waveform emitted from ferrites that must be addressed. First, the 1st wave in the comb-like structure is considerably weaker than the other subsequent signals, as is observed for the waveform measured by Antenna IV in Fig. 2(b). Second, in the waveform measured by Antenna IV, the intensity of the even-numbered waves (2nd or 4th waves) is much larger than that of the odd-numbered waves (3rd or 5th waves). The first observation can be explained by examining the relation between the acoustically excited area and the signal intensity. In this experiment, the ultrasonic beam is focused into a spot with an area of about $\pi(0.7)^2$ mm^2 on the front face of the sample. The beam spreads out on the back face because of the refraction at the boundary between ferrite and water, resulting in the enhancement of the signal intensity. Assuming that the excitation area spreads on the back face by a factor of S and the acoustic power per unit of area is reduced by a factor of $1/S$, the acoustic pressure should be reduced by a factor of $1/\sqrt{S}$ on the back face. If the amplitude of the acoustically modulated rf magnetic flux density, B, is proportional to the acoustic pressures, the modulated total flux, Φ, should be expressed as a function of $1/\sqrt{S} \times S = \sqrt{S}$. Because the signal voltages, V_{sig}, of the ASEM response detected by a loop antenna are expressed by $V_{\mathrm{sig}} = -d\Phi/dt$, the signal intensity on the back face should be enhanced by a factor of $\sqrt{S}$. In this experiment, the convergent angle of the incident waves is approximately 7° and the refracting angle of the longitudinal waves in the ferrite is about 30°. Therefore, the excited area on the back face is calculated to be about $\pi(5.7)^2$ mm^2. The ratio of the area on the front face to that on the back face indicates the enhancement factor on the back face is about 8. Even though this is a rough analysis, it is broadly consistent with the experimental enhancement factor of 4. Next, we discuss why the intensity of even-numbered waves is enhanced in the experimental data measured by Antenna IV. The even-numbered waves are emitted from the back face (bottom surface) of the specimen, whereas the odd-numbered waves are emitted from the front face (upper surface). In the configuration for Antenna IV, the back face of the specimen is closer to the antenna. As described in Sec. II, the near-field component of the magnetic fields is detected in our measurements. Therefore, the signal intensity is inversely proportional to the cube of the distance. The ratio of the cube of the distance between the front and the back faces is about 2 in the Antenna IV configuration, which is consistent with an intensity ratio of 1.7.

V. MAGNETIC IMAGING THROUGH ASEM RESPONSE

We performed magnetic imaging via acoustic excitation (Fig. 3(a)). The measured samples are a pure iron foil (0.1 mm thick), a copper foil (0.2 mm thick) and a flake of ferrite magnet (SrO/6Fe$_2$O$_3$). The samples are positioned on the bottom of a glass beaker and the ASEM signals are detected by Antenna IV. The pulse width of the detected ASEM waveform is less than 0.5 μs, indicating that the local ASEM response is mapped. The lateral spatial resolution is determined by the spot size of the focused ultrasonic beam (~0.7 μm). Well-defined signals from the ferrite and weak radiation along the sample edges of the pure iron foil are observed. Figure 3(b) shows the detailed profiles of the ASEM imaging for pure iron foil, suggesting the presence of magnetization along the sample edges. Because net radiation is not expected in the magnetic multiple domains of iron, we assume that the signal arises from the aligned domains induced by external stress or distortion when the iron foil is cut. When an external distortion is applied by folding the foil in the middle, radiation is observed along the folded line (Fig. 3(c)).

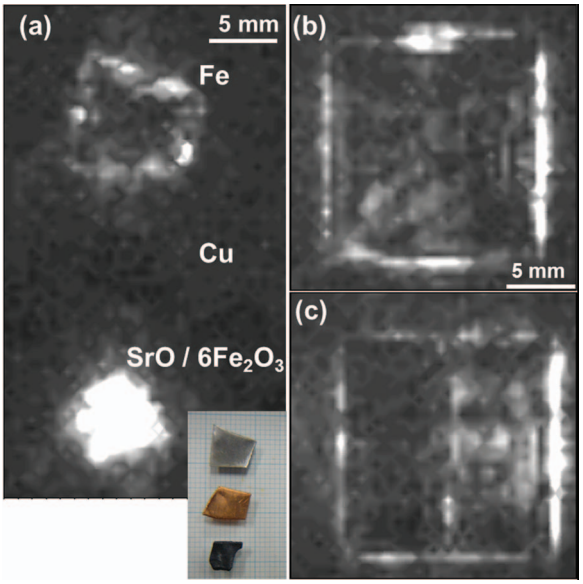

FIG. 3. (a) Magnetically selective ultrasonic imaging using the ASEM response. The white regions indicate a higher ASEM intensity. The inset is a photograph of the samples (iron and copper foils, and a flake of SrO/6Fe$_2$O$_3$). ASEM images of the iron foil (b) before and (c) after folding.

Downloaded 02 May 2013 to 142.51.1.212. This article is copyrighted as indicated in the abstract. Reuse of AIP content is subject to the terms at: http://rsi.aip.org/about/rights_and_permissions

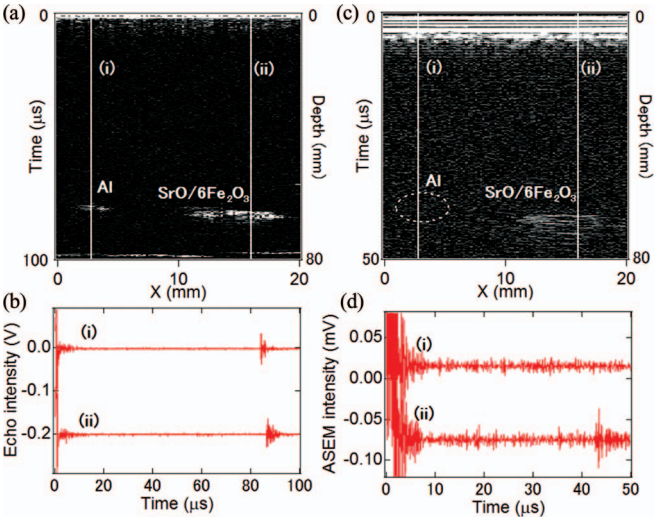

FIG. 4. Demonstration of ASEM tomography. (a) Several foreign materials in a gel phantom detected by conventional ultrasonic pulse-echo tomography. (b) The real-time waveform of the echo signals at two positions, indicated by the white lines (i) and (ii) in (a). (c) ASEM tomography, measured simultaneously with the echo measurements, can distinguish the ferromagnetic materials from the foreign materials. Nonmagnetic materials (Al) are not detected by ASEM tomography. (d) Real-time waveform of the ASEM signals.

The tomographic imaging of the ASEM response is shown in Fig. 4. Several flakes of nonmagnetic aluminum and magnetic ferrite are implanted into a gel phantom. The depth resolution is comparable to that of echo inspection (∼0.2 mm). Magnetic flakes (ferrites) are easily distinguished in ASEM tomography (Figs. 4(c) and 4(d)), whereas all flakes appear similar in the echo measurements (Figs. 4(a) and 4(b)). Therefore, the ASEM method can be used for evaluating whether foreign materials are ferromagnetic or not.

VI. DETECTION OF STRAIN-INDUCED MARTENSITIC TRANSFORMATION

In this section, we present an example of metal inspection using the ASEM response. Austenitic stainless steels show a strain-induced transformation from the austenitic phase to the ferromagnetic martensitic phase when plastic deformation occurs.[7] Sensing the plastic deformation or the dynamical process through magnetic imaging is a potential approach to detecting metal embrittlement.

Figure 5 shows the correlation between the ASEM intensity and the surface magnetic flux density, B_s. Six stainless steel plate specimens (size: 9.9 × 26.4 × 0.5 mm) are subjected to an external field of about 1 T for about 10 s before the measurements. The field strength comparable to the coercive force will be needed for producing residual magnetization, and it is normally smaller than 0.1 T for iron-based alloys.[10] Spatial images of the ASEM response in austenitic stainless steel are shown in Fig. 5(a). In the non-stressed sample (left panel, Fig. 5(a)), ASEM signals are observed along the sample boundary only. This indicates that residual magnetization is generated when the sample is manufactured. The distribution of the magnetization extends to the central part of the plate for the specimen stressed at 600 MPa (right panel,

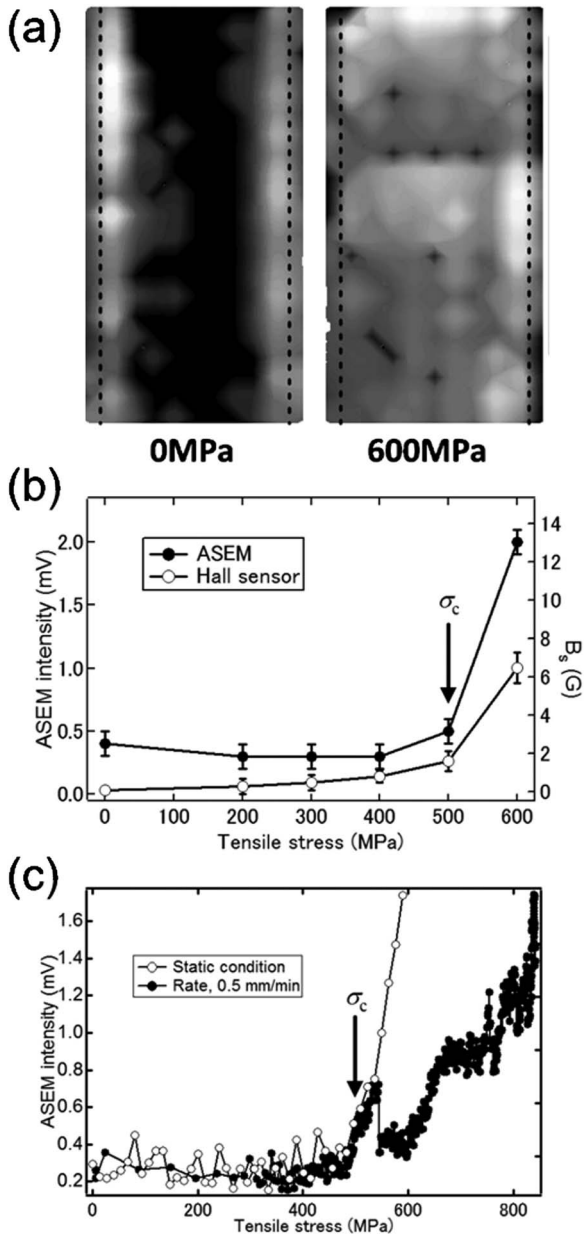

FIG. 5. (a) ASEM images of austenitic stainless steels before (left) and after plastic deformation (right). (b) The correlation between ASEM intensity and surface magnetic flux density, B_s. The arrow indicates the critical stress value, $\sigma_c \simeq 500$ MPa, as reported in Ref. 7. (c) *In situ* observation of the martensitic transformation during the tensile testing process. The specimens are placed in a tensile testing machine and in contact with a water-mediated ultrasonic probe. A magnetic field is applied with a permanent magnet during measurements. A loop antenna is placed so as to detect rf magnetic fields induced through d_{3m}, which corresponds to Antenna IV in measurements of ferrite magnets. The open and closed circles represent experimental results under static conditions and during dynamical processes at a constant extension rate of 0.5 mm/min, respectively.

Fig. 5(a)). Thus, we focus on the magnetic characteristics of the central part of the plate.[11] Figure 5(b) shows that the martensitic transformation is detected well by the ASEM response. Here, the signal-to-noise (SN) ratio at 600 MPa is about 10 with an integration time of 50 s and a pulse repletion rate of 2 kHz. The sensitivity (noise equivalent field) normalized by the integration time is estimated to be about 6 G/Hz$^{1/2}$. Because the measurement time is limited to the processing

Downloaded 02 May 2013 to 142.51.1.212. This article is copyrighted as indicated in the abstract. Reuse of AIP content is subject to the terms at: http://rsi.aip.org/about/rights_and_permissions

capability for waveform acquisition, the effective sensitivity could be further improved by introducing a specialized faster analog-digital convertor.

We also observe the martensitic transformation of austenitic stainless steel mounted on a tensile testing machine *in situ*. The sensitive measurements are carried out on a factory floor with careful attention to the ground lines and local rf shielding. The ASEM intensity, V_{sig}, as a function of the external tensile stress measured in the machine, σ_{ex}, is shown in Fig. 5(c). For the static measurements, each experimental point is measured until the ASEM intensity stabilizes, typically after about 3 min. The experimental results for the static measurements (open circles in Fig. 5(c)) correspond well to those of laboratory measurements shown in Fig. 5(b). Furthermore, the onset stress obtained from the dynamical measurements at a constant extension rate of 0.5 mm/min (closed circles in Fig. 5(c)), agrees with the critical value, σ_c. However, the V_{sig} drops at 550 MPa and increases again with a rise in stress although no significant change is observed in the ultrasonic pulse-echo signals measured at the same time. We interpret the dynamical behavior as follows. In the elastic regime, the balance of stress will be maintained even in the dynamical process (i.e., $\sigma_{ex} \simeq \sigma_{int}$, where the σ_{int} is the internal stress of the specimen). The dynamical behavior will be in agreement with the results under the static condition. This is supported by the results (closed circles) in Fig. 5(c) below the critical value, σ_c. In the plastic regime above the σ_c, however, the balance of stress is not required in the dynamical process; the internal stress will be released when the ferromagnetic martensitic domain (i.e., plastic deformation region) spreads out across the sample cross-section perpendicular to the tensile direction. Assuming that $V_{sig} \propto B_s \propto \sigma_{int}$, the decrease of internal stress will cause the ASEM intensity to decrease in the dynamical process. The drop of the V_{sig} thus indicates the onset of plastic deformation across the cross-section of the stainless steel plate.[12]

VII. CONCLUSION

We have demonstrated the magnetic measurements of ferromagnets by using acoustic excitation. Magnetization was visualized through the ASEM response using the sensitive rf detection with a narrowband loop antenna tuned to an ultrasonic frequency of 10 MHz. We confirmed that the longitudinal acoustic excitation induced the rf amplitude modulation of the residual magnetization, providing that the geometric configuration of antenna was correct. The ferromagnetic materials were selectively imaged with a spatial resolution of less than 1 mm through ultrasonic scanning. We showed that the ASEM tomography combines good acoustic resolution with magnetic contrast and can be used in combination with the conventional pulse-echo inspection.

Significant improvement of the lateral spatial resolution will be expected by combining the ASEM techniques with a high-frequency ultrasonic microscope, which may be used for microscopic studies of magnetic functional materials. ASEM tomography inherits limitations from the penetration depth of EM radiation. It is suitable for nonmetallic soft matter with an inhomogeneous magnetic distribution. It may be possible, however, to apply ASEM tomography to conducting materials where the ASEM signals are converted to lower frequencies through nonlinear acoustic effects.[13]

The ASEM method was also used for detecting the strain induced martensitic transformation in austenitic stainless steels. In our current measurement setup, the effective sensitivity for surface magnetic flux density was estimated to be about 6 G/Hz$^{1/2}$. The *in situ* observation of the martensitic transformation was achieved by introducing the measurement setup to a tensile testing machine. An anomalous ASEM intensity peak was observed in the dynamical measurements of tensile testing, suggesting the temporal release of the internal stress through the plastic deformation.

ACKNOWLEDGMENTS

This work is financially supported by Grant-in-Aid for Scientific Research (Grant No. B22360037).

[1]A. M. Chang, H. D. Hallen, L. Harriott, H. F. Hess, H. L. Kao, J. Kwo, R. E. Miller, R. Wolfe, and J. van der Ziel, Appl. Phys. Lett. **61**, 1974 (1992).
[2]L. N. Vu, M. S. Wistrom, and D. J. Van Harlingen, Appl. Phys. Lett. **63**, 1693 (1993).
[3]M. Oka, T. Yakushiji, and M. Enokizono, IEEE Trans. Magn. **37**, 2045 (2001).
[4]M. Cohen, IEEE. Trans. Magn. **1**, 156 (1965).
[5]For instance, W. K. Hiebert, A. Stankiewicz, and M. R. Freeman, Phys. Rev. Lett. **79**, 1134 (1997).
[6]K. Ikushima, S. Watanuki, and S. Komiyama, Appl. Phys. Lett. **89**, 194103 (2006).
[7]B. G. Koepke, R. P. Jewett, and W. T. Chandler, Nature (London) **210**, 1252 (1966).
[8]D. A. Berlincourt, D. R. Curran, and H. Jaffe, *Physical Acoustics* (Academic Press, New York/London, 1964), Vol. 1(Pt. A), pp. 169–270.
[9]J. D. Jackson, *Classical Electromagnetism*, 3rd ed. (Wiley, USA, 1998), pp. 413–416.
[10]K. Mumtaz, S. Takahashi, J. Echigoya, Y. Kamada, L. F. Zhang, H. Kikuchi, K. Ara, and M. Sato, J. Mater. Sci. **39**, 85 (2004).
[11]The central part of the plates is irradiated with the pulsed ultrasonic beam. The extra signals from the sample boundary are removed by checking the deviation from the $t_{echo}/2$ of the pulsed ASEM signals.
[12]S. S. Hecker, M. G. Stout, K. P. Staudhammer, and J. L. Smith, Metall. Trans. A **13**, 619 (1982).
[13]P. J. Westervelt, J. Acoust. Soc. Am. **35**, 535 (1963).

Downloaded 02 May 2013 to 142.51.1.212. This article is copyrighted as indicated in the abstract. Reuse of AIP content is subject to the terms at: http://rsi.aip.org/about/rights_and_permissions